Final

INTEGRATED ENVIRONMENTAL MONITORING SYSTEM FOR SPACECRAFT

A. Bogorad, C. Bowman, A. Dennis, J. Beck, D. Lang, and R. Herschitz
Lockheed Martin Astro Space
P*O, Box 800
Princeton, New Jersey 08543

Martin Buehler and Brent Blaes
Jet Propulsion Laboratory, California Institute of Technology
4$00 Oak Grove Drive
Pasadena CA 91109

Dennis Martin
Halcyon Microelectronics, Inc.
5467 Second Street
Irwindale, CA 91706

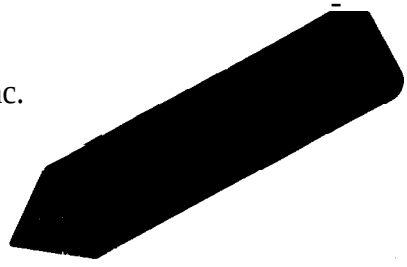

1, ABSTRACT

This paper describes an integrated space environmental monitoring system for geosynchronous satellites, The system provides measurements of surface charging, internal charging, and total dose radiation from the space environment, This system has been installed on one of Martin Marietta's commercial communications spacecraft, which is scheduled for launch in the near future. There are two components: an integrated charge monitor; which provides total dose and internal charging flux information, and a surface charge detector. Weight is less than one pound; power consumption, about 0,5 watts, Charging flux information from these detectors will permit evaluation of the effects of internal charging on electronic PC boards and will lead to the development of reliable, low-weight methods to detect on-orbit spacecraft charging events and to control charging and discharging.

2, INTRODUCTION

The uncertainties in predicting the effects of energetic particles on satellite systems remain a concern to all spacecraft designers and users, To assist the development of effective mitigation techniques, a lightweight, low-power monitoring system has been designed and built by Martin Marietta Astro Space (now a division of Lockheed Martin) and Jet Propulsion Laboratory, The system consists of two types of instruments -- (1) a radiation dosimeter calibrated to measure internal charging and (2) a surface charging detector, Both instruments will produce continuous telemetry data throughout the mission.

The system will provide a means of monitoring external and internal charging events aboard satellites, which will be very useful in determining the effectiveness of surface ESD control measures, such as conductive coatings, and of protective measures, such as grounded metal shielding, developed for mitigating internal charging effects on PC boards and cables. These evaluations will point the way to future design solutions and to the development of realistic design requirements for control of surface charging and internal charging.

The surface charging monitor was designed to measure charging by magnetospheric plasma electrons with energies from 5 keV to 20 keV and with worst-case current density from 0.1 to 1 nA/cm^2. The charge monitor will indicate when such an environment is present at the spacecraft's orbital location, Two of these units have been mounted in different places On one of Martin Marietta's commercial communications satellites scheduled for launch in the near future.

Post-it™ Fax Note 7671	Date	# of pages ▶
To M. Buehler ✓	From A. Bogorad	
Co./Dept.	Co. Martin Marietta	
Phone # 354-4362	Phone # 609-490-3835	
Fax #	Fax #	

The internal charging detector was designed to monitor flux of, and total dose imparted by, electrons with energies from 200 keV to 6 MeV. This detector will indicate when such an environment is present at the spacecraft's orbital location and will measure the flux of these electrons at various locations inside the spacecraft structure. The key component is a dosimeter designed, fabricated, and tested by the Center for Space Microelectronics Technology, Jet Propulsion Laboratory of the California Institute of Technology [1, 2]. Two of these units have also been mounted on the Martin Marietta satellite.

3. DESIGN DESCRIPTION

3.1. Surface Charging Detector

The surface charge detector has two components -- the charging plate and the associated control electronics, The charging plate is mounted to the spacecraft structure outside the spacecraft and is exposed directly to the space environment, The control electronics unit operates from the +/-15 volt power lines, It is located inside the spacecraft with the charging plate connected to the input of the instrumentation operational amplifier through a high-input- impedance buffering RC circuit as shown in Figure 1, The operational amplifier was configured to provide a 0- to 5-volt output compatible with the standard telemetry format.

Three critical choices during the design of the detector were: charging plate surface material, charging plate substrate, and mounting adhesive. The selection parameters for the surface material and mounting adhesive included electrical conductivity, high voltage leakage current, thermal expansion coefficient, thermo-optical properties, and space environmental stability in the operational temperature range, Surface materials that were considered for the charging plate included S13GLO white paint, Z306 Chemglaze black paint, black anodize, and alumina. Adhesives included RTV 566, CV2946, CV2943, and alumina-loaded Solithane 113. All candidate surface materials and adhesives were tested in a monoenergetic electron beam for their charging potentials, charging and discharging time constants, and compatibility with the readout circuits. A detailed description of the test procedure and test facilities is given in [3-5]

The result of the selection process is a charge collector in the form of a 2" by 2" aluminum plate painted with Chemglaze 2306 dielectric paint bonded to the spacecraft with non-conductive CV2946 adhesive. The plate is charged by impinging electrons The charging potential on the painted surface can vary from slightly positive to several hundred volts negative, with a corresponding potential on the underlying aluminum plate varying from +5 to -25 volts. This is the result of dividing the surface-to-ground voltage between the two series capactiors in Fig. 1.

The sensor was calibrated with 5-KeV, 10-KeV, and 20-KeV electron beams (beam current densities from 0.25 nA/cm 2 to 1 nA/cm 2) over a -400 C to 600 C temperature range. Typical calibration curves are shown in Figure 2. Several qualification tests were performed on all sensors prior to their integration into the spacecraft. These tests included radiation testing (400 megarads total dose) and thermal cycling (5000 cycles from +60° C to -600 C) on the charge plate; also radiation testing to a total dose of 30 kilorads on the readout circuit. ESD and DC overvoltage tests were also conducted on the readout circuit.

3.2. Dosimeter/Internal Charge Monitor

The dosimeter within the charge monitor comprises four identical radiation-sensitive p-FETs each shielded with a different-thickness Kovar lid. The thinly shielded transistors correspond to components near the surface of a spacecraft; the thickly shielded transistors, to components deep within the spacecraft Shield thicknesses were selected by trading FET lifetime vs. sensitivity to dose. The directly sensed quantity is ON-channel voltage drop at the temperature-independent current. This is related by calibration to total dose. Total dose can then be related by calculation to incident electron fluence. Differentiating the fluence with respect to time gives charging flux.

The outermost transistors have a higher charge rate, which leads to better resolution, but, since the ON-channel voltage drop saturates at a certain total dose, this also leads to shorter lifetime. That is, the outermost transistors will probably saturate. before the end of the satellite's mission,

The microchip layout developed on this effort is shown in Figure 3. It consists of seven components listed in Table 1 including p-FETs PO, PI, P2, and P7, each with different shields. These shields were fabricated in the Kovar lid by chemical etching. The microchip, shown in Fig. 3, was fabricated in a 1.2-µm CMOS rad-soft process, The chip was packaged in a 16-pin flat pack. The equivalent circuit for the chip, shown in Fig. 4, has a multiplexer and decoder used to place each component selectively in the feedback loop of the operational amplifier circuit shown in Fig, 5. The circuitry was designed to force a current at the temperature independent point through the p-FET during measurement. When not operating, the p-FETs are unbiased.

The calibration of the p-FET must account for both dose and temperature effects, The analog voltage, VA, shown in Fig, 5 is :

$$VA(T, D) = VA_{oo} + VA_T(T - To) + VO_D \cdot G \cdot D \quad (1)$$

where VA_{oo} is the initial output voltage determined from ground tests, VA_T is the temperature coefficient determined from g-round test data, VO_D is the dose coefficient determined from Co-60 ground tests, G = Gain = R13/R12, and $To = 27^{o}C$. D is the dose in kilorads; T is the temperature in K. The dose is calculated from :

$$D = [VA - VA_{oo} - VA_T(T - To)]/(VO_D \cdot G) \quad (2)$$

The output voltage, VO, for the p-FET follows from the square 1 aw behavior of the FET operating in saturation [11:

$$VO = VT - (2 \cdot ID/\beta)^{1/2} \quad (3)$$

where VT is the threshold voltage, β is the tranconductance, and ID is the drain current chosen at the temperature independent point. This expression is used to determine the VO-dose calibration curve given VT, β, and ID as discussed below.

The temperature-dose expression for the VT is:

$$VT = VT_{oo} + VT_T \cdot (T - To) + \Delta VT[1 - \exp(-D/Do)] \quad (4)$$

where VToo is the threshold voltage at To and D = f), VT_T is the threshold voltage temperature coefficient, Do is the VT dose coefficient, and ΔVT is the maximum change in VT when the radiation reaches infinity, When D= Do and at constant T, the VT increases by ΔVT[1-1/e]. The expression for VT indicates that VT is rate limited, which depends on the filling of a finite supply of gate-oxide hole traps [6], The VT equation was solved using the least-squares method to determine VT_{oo}, VT_T, and ΔVT. The parameter Do was found using an optimization technique that maximizes the least-squares correlation coefficient.

The dose-temperature expression for β is :

$$\beta = \beta_{oo}(T/To)^{-n}/[1 + (D/Dm)(T/To)^{-n}] \quad (5)$$

where βoo is β evaluated at To and D=0, n is the β temperature coefficient and Dm is the β or mobility dose coefficient, When D = Dm at T= To, then β is reduced by 50%. This equation was formulated by combining the β temperature and dose dependence as the sum of reciprocals.

The p-FET drain current at the temperature independent operating point, IDm, is found by differentiating the VO expression with respect to temperature. Setting the resulting expression equal to zero at the measurement temperature, Tm (which is the expected on-orbit operating temperature), and D=0 leads to [61:

$$IDm = 2(\beta mo)^{3}(-VTT/\beta Tmo)^{2} \qquad (6)$$

where $\beta Tmo = (-n/Tm)\beta mo$, $\beta mo = (Tm/To)^{-n}$.

The VT, β, and VO results are presented graphically in Figs. 6 to 8. 'f'he curves were obtained by fitting the data shown in Fig. 6 to Eq. 4 and the data shown in Fig. 7 to Eq. 5. Thus, the p-FET results can be characterized by seven parameters, namely VToo, VTT, ΔVT, Do, βoo, n and Dm. These parameters are listed in Table 2 for transistor P0. The device-to-device uniformity was excellent,

VO values were obtained from Eq. 3 using Eq. 4 for VT, Eq. 5 for β, and Eq. 6 for IDm. The VOmo values listed in Table 5 for each of the four p-FETs, are within 0,1% of each other. The VO values are plotted in Fig. 8 for two different values of IDmo. The curves for the P0 design value of IDmo = 88 μA show that VO is fully temperature compensated at D=0. The curves for the operating value IDmo=1 00 mA show that temperature compensation occurs near 100 krads and that VOmo=1.57 V, These parameters were used as the target design parameters, thus the 100 mA curve is designated as the calibration curve. The samples from the flight lot of dosimeters were radiation tested and calibrated using a Co-60 gamma source at -25C, + 10C and 45 C. A burn-in test, centrifuging and temperature cycling tested were also performed on the flight devices,

A similarly fabricated p-FET was flown on STRV-1b, launched June 17, 1994 into a 10.59-hr orbit. The p-FET temperature dependence was determined from the slope of the flight data as shown in Fig, 9, The dose for the STRV-1b is shown in Fig. 10. It shows the dose at different locations and behind different shields in the JPL experiment box. The results indicate that dose is not uniform across the exposed portion of the box.

4. SPACECRAFT IMPLEMENTATION

As stated above, two surface charge monitors and two dosimeters have been installed on a Martin Marietta commercial communications satellite, Total weight of the system is less than one pound and it requires approximately 0.5 watts of power.

Surface charge monitors were installed on the north and anti-earth panels. The sensor located on the north panel will be continuously shadowed for a period of six months; then it will be continuously exposed to sunlight during the other six months; it will provide data on seasonal variations of spacecraft charging potential, The sensor mounted on the anti-earth panel will be moving in and out of the sunlight on the daily basis; it will provide data on daily variations in spacecraft charging potential.

In addition, two dosimeters will be used to monitor internal charging fluxes and total dose accumulation. One dosimeter was mounted on the north panel internal to the spacecraft structure with the sensor facing the panel, In addition to its Kovar lid, this sensor is shielded from external radiation by the spacecraft panel. This location is typical for most spacecraft components. The second dosimeter is located outside the spacecraft structure on the anti-earth

panel. In addition to the Kovar lid, this sensor is shielded from external radiation by a ten layer Kapton thermal blanket. Thus a total of eight p-FETs with different shield thicknesses will provide electron flux count in eight energy channels,

Support logic is combined with the sensors in order to meet the spacecraft's interface requirements, The sensors were tested for functional performance following their installation on the spacecraft and during spacecraft level thermal testing.

5. CONCLUSIONS

Development of mitigation techniques for spacecraft charging control requires thorough knowledge of the environmental conditions and of their impact on spacecraft components. an integrated space environmental monitoring system has been developed, built, and installed on a geosynchronous communications satellite, Its low weight and power requirements allow easy incorporation into the spacecraft design, satelli te performance can be correlated with in-situ charging and dose rate. Until now, the only environmental data available was from research satellites, in different time zones and along different flux tubes. We envision that in the future, such systems may become a standard part of the bus telemetry as common as temperature sensors for all geosynchronous spacecraft.

6. ACKNOWLEDGMENTS

This effort was sponsored by Martin Marietta's Independent Research and Development program and by the Ballistic Missile and Defense Organization, Innovative Science and Technology office. Dosimeters were developed and tested by the Center for Space Microelectronics, Jet Propulsion Laboratory, California Institute of Technology, The devices used in this study were fabricated through MOSIS, Information Sciences Institute, University of Southern California,

7. REFERENCES

[1] M.G. Buehler, "On-Chip p-MOSFET Dosimetry", IEEE Transactions on Nuclear Science and Space Radiation Effects, Vol. 40, No. 6,1442-1449 (1993).

[2] M.G. Buehler, G. A, Soli, B. R. Blaes, J. M. Ratliff, and H. B. Garrett, "Clementine RRELAX SRAM Particle Spectrometer", IEEE Transactions on Nuclear Science and Space Radiation Effects, Vol. 41, (1994),

[3] A. Bogorad, R. Herschitz and C. Bowman, " Environmental Stability of Low Absorptivity optical Solar Reflectors and Their Impact on Spacecraft Charging," IEEE Transactions on Nuclear Science and Space Radiation Effects, 41, No. 6, 1994.

[4] R. Herschitz, A. Bogorad and C. Bowman, "Space Environmental Testing of Blue Red Reflecting Coverglasses for Gallium Arsenide and High Efficiency Silicon Solar Cells," IEEE Conference Proceedings of First World Conference on Photovoltaic Energy Conversion, 1995.

[5]. A. Bogorad, C. Bowman, R. Herschitz, W. Krummann, and W. Hart, "Differential Charging Control on Solar Arrays for Geosynchronous Spacecraft", IEEE Transactions on Nuclear Science NS-40, 1320, (1993).

[6]. T. P. Ma and P, V, Dressendorfer, " Ionizing Radiation Effects in MOS Devices and Circuits", John Wiley, New York, 1989.

Table 1. Microchip Devices

DEVICE	TYPE	SHIELD (mil)
P0	GATE OXIDE p-FET	6
?1	GATE OXIDE p-FET	0
P2	GATE OXIDE p-FET	2
P7	GATE OXIDE p-FET	10
N3	FIELD OXIDE n-FET	not used
N5	GATE OXIDE n-FET	not used
R4	METAL-1 RESISTOR	70
E6	EXTERNAL DEVICE	NA

"l'able 2, P-FET Design Parameters

PARAMETER	DESCRIPTION	UNITS	VALUE
To	Reference value of temperature	^oC	27
Tm	On-orbit avalue of temperature	^oC	10
VToo	Threshold voltage @zero dose &To	V	-0.8598
VT_T	$\partial VT/\partial T$ at constant dose D	$mV/^oC$	1.7595
ΔVT	Saturation value of change in VT by dose D	V	-0,4998
Do	Value of D at which IVTI has increased by ΔVT[1-1/e]	kilorads	118,91
βoo	channel transconductance	$\mu A/V^2$	474.73
Dm	dose coefficient of β in eqn (5)	kilorads	588.5
n	temperature coefficient of β in eq. (5)		1.7196
IDmo	Design value of temperature-independent drain current	μA	prelim.: 88,36; final: 100
VOmo	Output voltage	V	prelim.: -1.47 final: -1.507

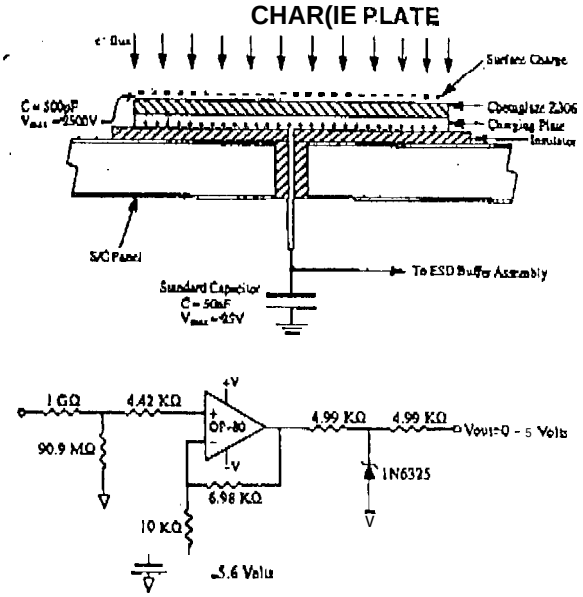

Figure 1. Surface Charging Sensor Description

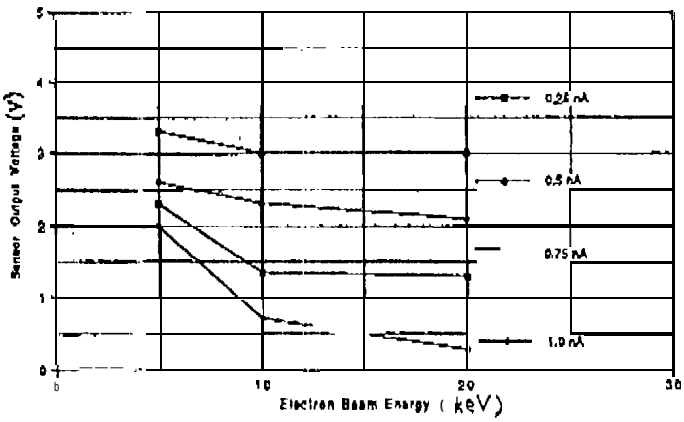

Figure 2. Surface Charging Sensor Calibration (T=25° C)

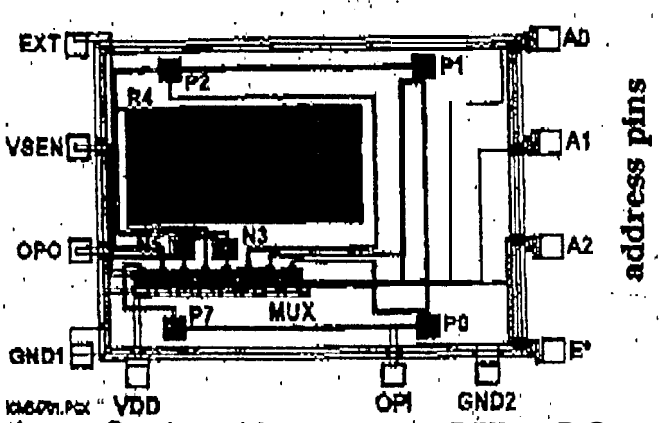

Figure 3. Microchip with four p-FETs, P0, P1, P2, and P7. Each p-FET is located behind a different shield whose thickness is listed in Table 1. The different shield thicknesses were obtained by selectively chem-etching the Kovar lid.

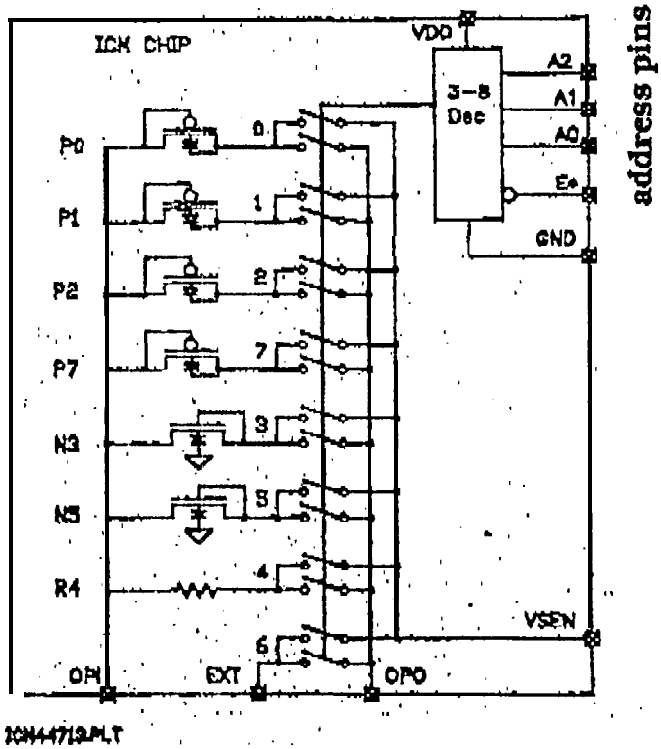

Figure 4. Microchip schematic.

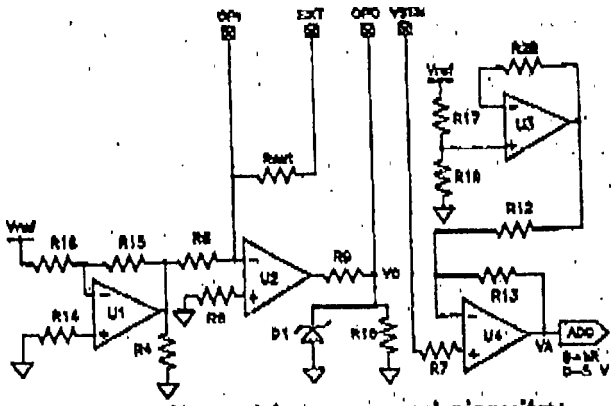

Figure 5. Microchip surround circuitry.

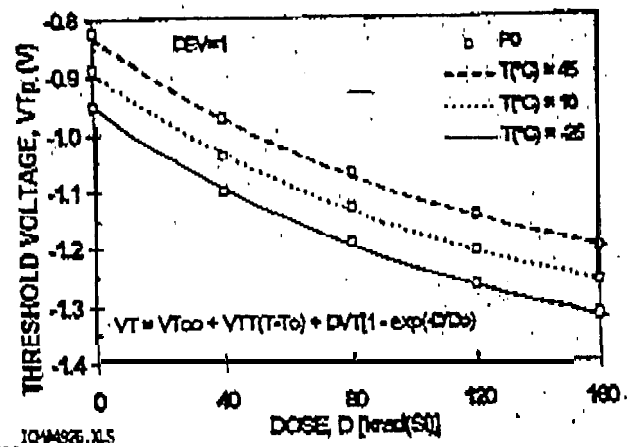

Figure 6. p-FET threshold voltage dose-temperature fit to Eq. 4.

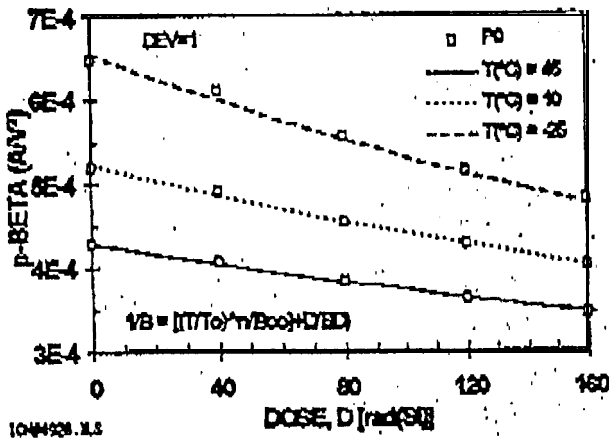

Figure 7. p-FET beta dose temperature fit to Eq. 5.

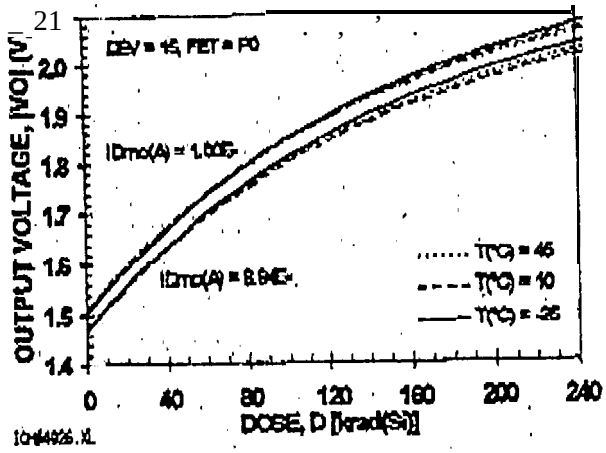

Figure 8. p-FET output voltage dose dependence.

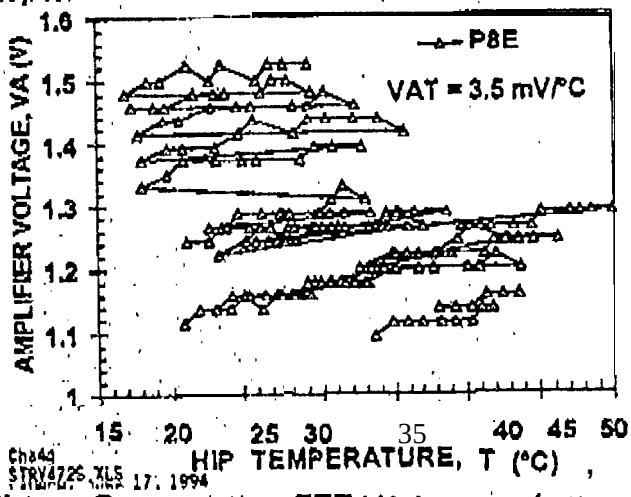

Figure 9. STRV-1b p-FET VA-temperature dependence, VA_T = 3.5 mV/°C.

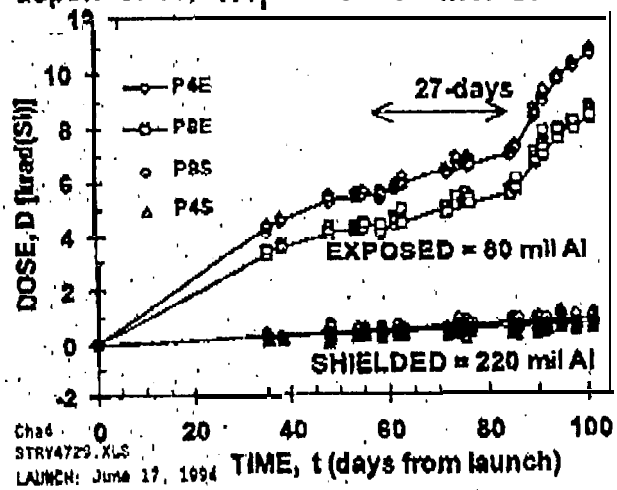

Figure 10. STRB-1b dose profile for devices behind 80-mm and 220-mm Al shields.